

# The humidity dependence of the maritime mist aerosol extinction coefficient and thermodynamic theory of solutions

A.N. Vulfson

*Institute of Oil and Gas Problems,  
Moscow State Institute of Electronics and Mathematics, Moscow*

Received March 15, 2001

Similarity theory and dimensional analysis are applied to construction of a relationship for the spectral aerosol extinction coefficient in the atmospheric window  $0.48 \cdot 10^4 < \lambda < 0.76 \cdot 10^4$  cm. The relationship is justified using the Mie theory. The results allow one to compare the *in situ* determined humidity dependence of the spectral extinction coefficient with available laboratory data on variation of the aerosol particle radius in the moist air. It is shown that the variations can be efficiently described in terms of the modified Raoult law for concentrated and moderately supersaturated solutions.

Coastal haze consisting of a great deal of droplets condensed on the particles of marine origin is a classic example of aerosol formation from inorganic soluble particles. Aerosol constituent of the haze is formed at destruction of small foam bubbles of near-coast waves<sup>1,2</sup> and has a composition close to the chemical composition of sea salt, i.e., 78% NaCl, 11% MgCl<sub>2</sub>, and 11% CaSO<sub>4</sub>, Na<sub>2</sub>SO<sub>4</sub>, and K<sub>2</sub>SO<sub>4</sub>. According to Ref. 1, the salt aerosol particles, remained at evaporation of sea haze droplets, have the greatest radius of  $40 \cdot 10^6$  cm with maximum distribution in the range  $10 \cdot 10^6$  to  $30 \cdot 10^6$  cm. It is reasonable to score the characteristic size of coastal haze particles on the general Junge scale of the atmospheric aerosol radii. According to Ref. 2, the total spectrum of atmospheric aerosol radii can be divided into three parts (Table):

(a) Aitken nuclei, lying in the range from  $0.5 \cdot 10^6$  to  $20 \cdot 10^6$  cm;

(b) large nuclei in the range from  $20 \cdot 10^6$  to  $1 \cdot 10^4$  cm;

(c) giant nuclei in the range greater than  $1 \cdot 10^4$  cm.

Thus, the coastal haze particles should be treated as a mixture of large condensation nuclei and the upper part of the spectrum of soluble Aitken nuclei.

Wright<sup>2,3</sup> was a pioneer in systematical experimental and theoretical studies of the effect of humidity on the coastal haze. Assuming that the number density of soluble nuclei in the moist air is constant and the particle spectrum is monodispersed, he has explained the decrease of visibility at the increase of humidity by a change of the aerosol particle size. The mean particle

radius was calculated provided that the sea salt solution droplet and water vapor are in thermodynamic equilibrium. Within the Wright approximation,<sup>2,3</sup> optical properties of coastal hazes are related to large soluble droplets. According to Refs. 2 and 3, the number density of large particles was  $63 \text{ cm}^{-3}$ , while their mass and mean radius were  $1.1 \cdot 10^{13} \text{ g}$  and  $2.3 \cdot 10^5 \text{ cm}$ , respectively.

In this paper, based on Wright's<sup>3</sup> and Hanel's<sup>4</sup> thermodynamic ideas, a sea haze particle is considered as a droplet of sea salt water solution only at the relative humidity higher than some threshold value. At lower values of the relative humidity, a sea salt particle is considered as a solution droplet containing a solid soluble core or as a droplet of supersaturated solution. The spectral Beer law is used to describe the spectral aerosol extinction coefficient of the sea haze in the visible atmospheric transparency window  $0.48 \cdot 10^4 < \lambda < 0.76 \cdot 10^4$  cm. The obtained results enable us to compare field observations of the humidity dependence of the spectral aerosol extinction coefficient<sup>5</sup> with the well-known laboratory observations of the aerosol particle radius variation in the moist air.<sup>6</sup> The use of more complete thermodynamic model of transformation of a droplet has shown that the humidity dependence of the aerosol extinction coefficient includes the ranges both of unambiguous and ambiguous humidity dependences, which have the hysteresis loop shape. Thermodynamic interpretation of the obtained results is suggested, which uses a modification of the Raoult law for concentrated and moderately supersaturated solutions.

Table

Characteristics of particles	Condensation nuclei					
	Aitken	Large	Giant			
Radius, cm	$0.5 \cdot 10^6$ $20 \cdot 10^6$	$20 \cdot 10^6$ $1 \cdot 10^4$	$1 \cdot 10^4$ $2 \cdot 10^4$	$2 \cdot 10^4$ $3 \cdot 10^4$	$3 \cdot 10^4$ $5 \cdot 10^4$	$5 \cdot 10^4$ $10 \cdot 10^4$
Mean number density of particles in $1 \text{ cm}^3$	42500	132	2.0800	0.0880	0.0244	0.0051
Mass, $\text{mg}/\text{m}^3$	17	26	23	4.2	5.1	9.1

### Formula for the extinction coefficient of the coastal atmospheric haze in the form of the spectral Beer law

The monochromatic flux  $J_\lambda$  passing through an optically dense layer of the atmospheric air of the thickness  $ds$  is attenuated due to absorption and scattering. According to the Bouguer law, this attenuation is proportional to  $J_\lambda$  and  $ds$ . Molecular absorption and scattering of light in the  $\alpha$ transparency windowB in the visible wavelength range are minimal and determined mainly by the presence of atmospheric aerosol.

The extinction coefficient of chemical and colloid diluted solutions is often proportional to its mole concentration. This phenomenological dependence is known as the Beer law.<sup>7</sup> Experimental dependence of the extinction coefficient  $\alpha_\lambda$  on the volume concentration  $c$  for water solution of  $Cu_2SO_4$  is shown in Fig. 1.

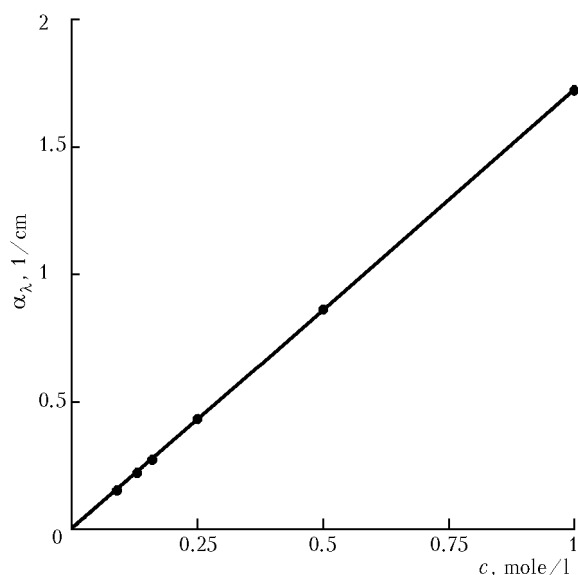


**Fig. 1.** Experimental confirmation of the Beer law for the water solution of  $Cu_2SO_4$ . The solution concentration is plotted along the horizontal axis, the extinction coefficient at the fixed wavelength  $\lambda = 0.6 \cdot 10^4$  cm is plotted along the vertical axis.

Consider the coastal haze as the solution of aerosol in air. Let  $\rho_a$  be the density of aerosol cloud,  $\rho$  is the density of air, and  $q_a = \rho_a/\rho$  is the aerosol mixture ratio. Based on dimensionality grounds, we modify the Beer law, introducing the dependence on the wavelength  $\lambda$  in the visible  $\alpha$ transparency windowB  $0.48 \cdot 10^4 < \lambda < 0.76 \cdot 10^4$  cm. Then, without loss of generality, we assume that the spectral formulae of the Bouguer and Beer laws take the form

$$\frac{dJ_\lambda}{ds} = -\alpha_\lambda J_\lambda; \quad \alpha_\lambda = \frac{3\pi a_{wc}^* \rho_a}{\lambda \rho}, \quad (1)$$

where  $\alpha_\lambda$  is the coefficient of aerosol monochromatic extinction, and  $3\pi a_{wc}^*$  is the constant numerical parameter.

To justify theoretically and experimentally the *a priori* introduction of the spectral Beer law (1), we transform its right part using statistical characteristics of the aerosol cloud.

Let  $\rho_{wc}$  be the characteristic density of aerosol particles, whose magnitude is close to the water density. Then the ratio of mixture of the system of monodispersed aerosol particles in air and the aerosol extinction coefficient take the form

$$q_a = \frac{\rho_a}{\rho} = \frac{4}{3} \pi \frac{\rho_{wc}}{\rho} N \tau^3; \quad \alpha_\lambda = \frac{4\pi^2 a_{wc}^* \rho_{wc}}{\lambda \rho} N \tau^3, \quad (2)$$

where  $\tau$  is the mean radius of an aerosol particle,  $N$  is the total number of particles of the aerosol cloud in the unit volume,  $\pi = 3.14\dots$

To justify Eq. (2) from the standpoint of physical optics, we assume that the light extinction is caused only by the effect of scattering. Let  $r$  be the radius of aerosol particle and  $N(r)dr$  is the number of particles in the range from  $r$  to  $r + dr$ . Consider the monodispersion spectrum  $N(r) = N\delta(r - \tau)$ , where  $\delta(r - \tau)$  is the Dirac delta-function. Then, according to the Mie theory<sup>7</sup> in the monodispersion spectrum approximation we obtain

$$\alpha_\lambda = \int_0^\infty \pi r^2 K(\xi) N(r) dr = \pi \tau^2 K\left\{\frac{4(m - 1) \pi \tau}{\lambda}\right\} N. \quad (3)$$

Here  $K(\xi)$  is the scattering efficiency factor, the function with known values,  $\xi = 4(m - 1) \pi r/\lambda$  is the diffraction parameter,  $m$  is the refractive index of an aerosol particle.

For the atmospheric haze consisting of the soluble Aitken nuclei, the mean radius  $\tau$  of a particle varies in significantly more narrow range than the entire spectrum of fine aerosol. In the variation range of the mean radius  $4 \cdot 10^6 < \tau < 40 \cdot 10^6$  cm, at the  $\alpha$ transparency windowB radiation in the visible wavelength range  $0.48 \cdot 10^4 < \lambda < 0.76 \cdot 10^4$  cm and the refractive index of water  $m = 1.33$ , the corresponding parameter  $\xi$  varies in the range  $0.22 < \xi < 3.45$ . It is important that  $K(0) = 0$ , and the first maximum of  $K(\xi)$  can be reached at  $\xi \approx 4$  (see Ref. 7). So, the linear dependence  $K(\xi)$  can be used as a rough approximation. It is well known that the refractive index of a solution depends on the density of a substance according to the Gladstone-Dale relationship.<sup>7</sup> Thus,

$$K(\xi) = \xi = \frac{4(m - 1) \pi \tau}{\lambda}; \quad (m - 1) = a_{wc}^* \frac{\rho_{wc}}{\rho}, \quad (4)$$

where  $a_{wc}^*$  is the dimensionless refraction coefficient. Taking into account all the aforementioned, the second formula (2), proposed earlier, follows from Eqs. (3) and (4).

Now we suggest the experimental reasoning of relationships (1) and (2). Considering atmospheric haze as a solution of aerosol in air, assume the parameters  $N$  and  $\rho_{wc}/\rho$  to be constant. Then it follows from formula (2) that the magnitude of  $\alpha_\lambda$  varies depending on the mean radius of aerosol particle  $r$ . According to Refs. 2 and 3, at a change of humidity,  $r$  varies so that the magnitude of the saturated vapor pressure on the droplet surface coincides with the water vapor pressure in air. Otherwise, the processes of evaporation and condensation necessarily would change the droplet radius. Thus, instead of the function (2) of the mean radius, it is possible to consider the dependence of the aerosol extinction on humidity.

The field data<sup>5</sup> on the dependence of the extinction coefficient on humidity in the coastal sea haze are shown in Fig. 2.

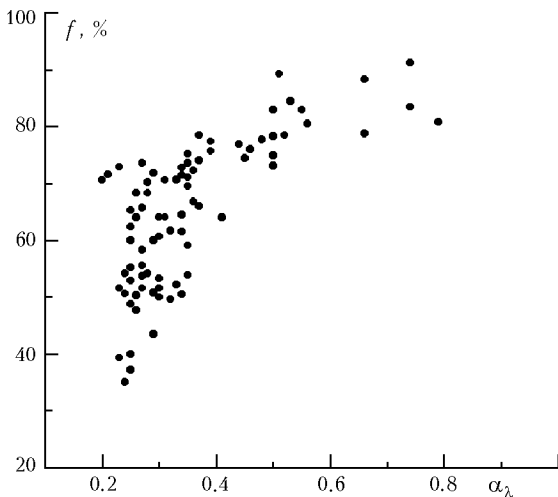


Fig. 2. Extinction coefficient  $\alpha_\lambda$  as function of humidity  $f$  in sea coastal haze from the data of Ref. 5 ( $\lambda = 0.48 \times 10^4$  cm).

On this basis, for the experimental reasoning of formula (2), it suffices to illustrate the agreement between Eq. (2) and field observations:

- (a) at variable wavelength  $\lambda$  and constant humidity  $f$ ;
- (b) at constant wavelength  $\lambda$  and variable humidity  $f$ .

The experimental data<sup>1</sup> confirming the hyperbolic dependence of the aerosol extinction coefficient (2) on  $\lambda$  at fixed humidity  $f$  are shown in Fig. 3.

Now we consider the possibility of experimental reasoning of the relationship (2) at fixed  $\lambda$  and variable  $f$ . Assume parameters  $n$  and  $\rho_{wc}/\rho$  to be constant, then it follows from Eq. (2) that

$$\alpha_\lambda^* = \frac{\alpha_\lambda(f)}{\alpha_\lambda(f_s)} = \frac{r^3(f)}{r^3(f_s)} = r_*^3, \quad (5)$$

where  $f_s$  is some fixed value of relative humidity,  $\alpha_\lambda(f_s)$  and  $r(f_s)$  are the aerosol extinction coefficient and the effective radius of aerosol particle, respectively, at the fixed value of  $f_s$ ;  $\alpha_\lambda^*$  and  $r_*$  are the dimensionless values

of the aerosol extinction coefficient and radius. It is essential that the relationships in right- and left-hand sides of Eq. (5) can be changed independently. The coincidence of the data obtained experimentally confirms Eq. (5), and, hence, the initial Beer relationship (2).

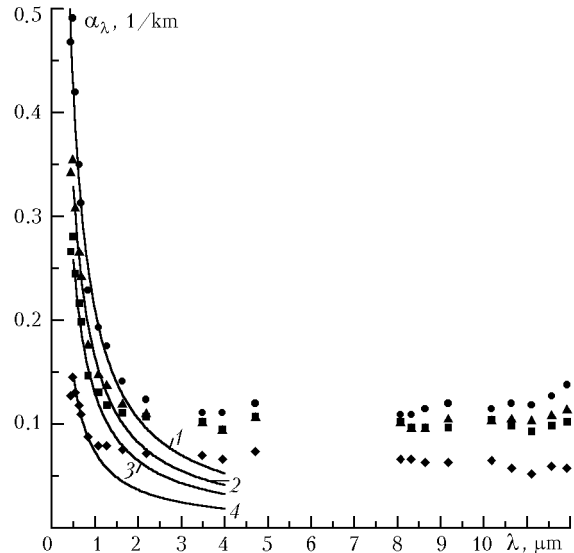


Fig. 3. Experimental data on the dependence of the extinction coefficient  $\alpha_\lambda$  on the wavelength  $\lambda$  at different values of relative humidity according to Ref. 1 (marked by signs). Hyperbolic approximations of the aerosol extinction coefficient on the wavelength  $\lambda$  at fixed values of humidity  $f$  are drawn by solid lines. Curve 1 corresponds to 93%, 2 to 84%, 3 to 76% and 4 to 60%.

### Experimental evidences and thermodynamic theory of change of radius of a water droplet containing a solid soluble Aitken nucleus, depending on variations of humidity

Laboratory investigations of the change of the solution droplet containing a solid soluble core depending on variations of humidity were described in Ref. 6. The solid crystal of NaCl with the effective radius  $a = 2.74 \cdot 10^6$  cm was placed into the atmosphere of moist air. Measurements of the equilibrium droplet radius were carried out at preset values of air humidity. The experimental results are shown in Fig. 4a.

As humidity increases (the interval  $AB$ ), the adsorption process occurs on the surface of a soluble particle. It practically does not change the initial radius of a dry crystal. As humidity reaches some threshold value (the point  $B$ ), covering the crystal with a water film starts, and the crystal partially dissolves in it forming a saturated solution. Thus (in the interval  $BC$ ) the radius of the solution droplet, containing a solid soluble core, monotonically increases almost without changing the humidity of air. In the point  $C$  the crystal

is completely dissolved forming a droplet, the radius of which is approximately twice as large as the radius of a dry crystal. Further increase of humidity leads to the increase of the equilibrium radius of the solution droplet (the interval *CD*). Of prime interest should be the experiments, which deal with successive decrease of humidity. As humidity decreases, the droplet radius begins to decrease (the interval *DC*). However, when the point *C* is reached, a solid crystal is not formed inside the droplet. As humidity decreases, the supersaturated solution exists up to the point *E*. When this threshold value is reached, the droplet of the supersaturated solution is crystallized to the initial radius of the dry crystal practically without change of humidity (the interval *EA*). Thus, the curve of changing the radius of a droplet containing a solid soluble core, changes variously depending on the increase or decrease of humidity, i.e., the directed change of humidity forms the hysteresis loop. The realistic pattern (by the data of Ref. 6) of changing the radius of a droplet containing the NaCl solid soluble crystal with radius  $a = 2.74 \cdot 10^{56}$  cm is shown in Fig. 4*b*.

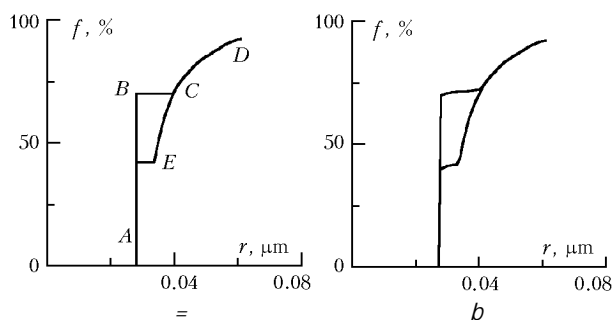


**Fig. 4.** The change of the radius of droplet *r* containing the solid soluble core as function of humidity *f*: schematic pattern of the process of adsorption, dissolving, and crystallization (a), experimental data on moistening the crystal of NaCl of the radius  $a = 2.74 \cdot 10^{56}$  cm (b).<sup>6</sup>

It is important that the profile *ABCDE* is consistent with thermodynamic theory. The curve *CDE* can be calculated by the Keller model<sup>2</sup> describing the saturated vapor pressure above the droplet. Profile *AB* is determined with high accuracy when solving the problem on the saturated vapor pressure above the solution droplet containing a solid soluble core.<sup>8,11</sup> Profile *BC* can be calculated from the condition of thermodynamic stability of the solution droplet covering the solid core.<sup>9</sup>

### Comparison of experimental data on variations of the extinction coefficient and the effective radius of an aerosol particle

To justify experimentally the proposed form of the Beer law (5), we represent the field observations<sup>5</sup> shown in Fig. 2 in a new coordinate system. We plot

the value of relative humidity *f* along the vertical axis, and the value  $(\alpha_\lambda^*)^{1/3}$  along the horizontal axis, assuming in Eq. (5) that  $f_s = 75\%$ ,  $\alpha_\lambda(f_s) = 0.45 \text{ km}^{51}$ .

The corresponding laboratory observations<sup>6</sup> (see Fig. 4*b*) are also represented in the new coordinate system. The value of relative humidity is plotted along the vertical axis, and  $r_*$  along the horizontal axis, assuming in Eq. (5) that  $f_s = 75\%$ ,  $\tau(f_s) = 4.2 \cdot 10^{56}$  cm.

Quite good agreement of the experimental points (Fig. 5) is the evidence of correctness of the relationship (5) and, hence, the validation of the form of the Beer law (2).

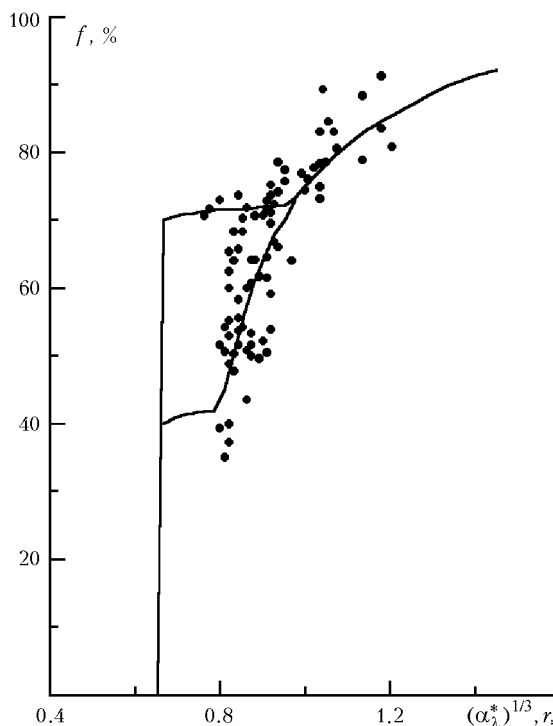


**Fig. 5.** Comparison of the dependences of experimental data on the dimensionless extinction coefficient  $(\alpha_\lambda^*)^{1/3}$  and dimensionless radius  $r_*$  on relative humidity *f*.

Note that the unambiguous dependence  $\alpha_\lambda(f)$  exists only at  $f > f_s = 71\%$ . There is no unambiguous dependence  $\alpha_\lambda(f)$  at  $f < f_s$ , because the humidity hysteresis results in scattering of experimental values of  $\alpha_\lambda(f)$  along the corresponding branches  $\tau(f)$ .

### Equation for state of concentrated and moderately supersaturated solutions and their vapor

Let  $v_w$  and  $v_{ws}$  be the specific volume of pure solvent and solvent in the solution, respectively. The approximation of the volume of saturated solution is used below. According to the approximation, the volume of concentrated and moderately supersaturated solutions is identified with the volume of saturated

solution (see Ref. 12 for greater detail). Assume that the soluble substance and solvent, like gas, occupy the entire volume. Taking into account the fact that the volume of saturated solution somewhat exceeds the volume of pure solvent, it is possible to write for concentrated and moderately supersaturated solutions

$$v_{WS} = k_{\infty} v_W, \tag{6}$$

where  $k_{\infty} = 1.11$  for the solutions of NaCl.<sup>10,12</sup>

The general Donnan-Guggenheim osmotic equation of state, generalized to the solution of electrolyte, has the form

$$\begin{cases} \pi^* v_W / R_W T = c \Phi(c, T), \\ \Phi(c, T) = (i_0 + i_1 c + i_2 c^2 + \dots). \end{cases} \tag{7}$$

Here  $\pi^*$  is the osmotic pressure,  $c$  is the mole concentration,  $\Phi(c, T) \geq 0$  is the osmotic coefficient, the non-negative function depending on the nature of the solution,  $i_n(T)$  are the functions fixed for each solution,  $R_W$  is the gas constant of water vapor related to the universal gas constant  $R$  through the relationship  $R_W = R / \mu_W$ , where  $\mu_W$  is the molecular mass of water.

The general osmotic equation of state (7) for concentrated unsaturated and moderately supersaturated solutions can be expanded by a Taylor's theorem in the vicinity of the saturation point  $c = c_{\infty}$ . Then

$$\frac{v_W}{R_W T} (\pi^* - \pi_{\infty}^*) = i_{\infty} (c - c_{\infty}), \tag{8}$$

where  $\pi^*$  is the osmotic pressure of the saturated solution above the plane surface of soluble substance,  $i_{\infty}(T) = \left. \frac{\partial}{\partial c} \Phi(c, T) \right|_{c_{\infty}}$  is some empiric function constant under isothermal conditions.

The value of  $c_{\infty}$ , corresponding to the concentration of saturated solution, is known from the solution Tables. The values of  $i_{\infty}$  and  $\pi_{\infty}^*$  can be determined from direct measurements of the osmotic pressure  $\pi^*$  or from the known values of the osmotic coefficient. Comparison of the experimental data<sup>10</sup> with the relationship (8) was performed in Refs. 8, 9, and 12. According to Refs. 8 and 9,  $\pi^* = 39.058$  MPa for the NaCl saturated solution at  $t = 20^{\circ}\text{C}$ ,  $c_{\infty} = 0.1109$ ,  $i_{\infty} = 3.40$  (Fig. 6).

Note that, although formula (8) is quite rough approximation of equation (7), nevertheless, as follows from Fig. 6, it is acceptable for concentrations in the range  $|c - c_{\infty}| / c_{\infty} < 0.4$ .

Obviously, at small deviations of concentration of a solution of an arbitrary chemical origin from saturation the following equation of state is also fulfilled:

$$\frac{v_W (\pi^* - \pi_{\infty}^*)}{R_W T} = i_{\infty} c_{\infty} \ln \frac{c}{c_{\infty}}. \tag{9}$$

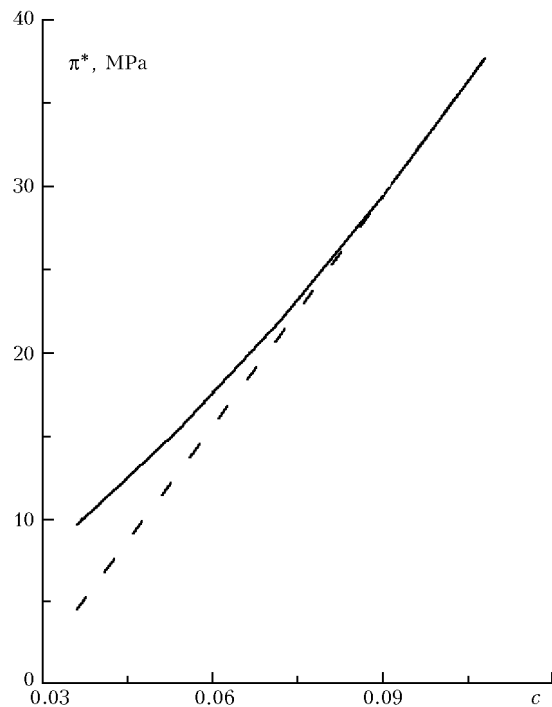


Fig. 6. Osmotic pressure  $\pi^*$  as function of the mole concentration  $c$  of the solution of NaCl at fixed temperature  $t = 20^{\circ}\text{C}$  from the data of Ref. 10 is shown by solid line. Dotted line shows the suggested approximation (8).

Further the equation of state in the form (9) is used for analytical description of transformation of spherical droplets of solution in the atmosphere of moist air, as well as for calculation of the aerosol extinction coefficient.

Under natural conditions water can be evaporated from the solution forming water vapor. Assume that the saturated vapor of atmospheric air fulfils the ideal gas equation of state, i.e.,

$$E v_v = R_W T, \tag{10}$$

where  $v_v$  and  $E$  are the specific volume and the pressure of the saturated water vapor, respectively.

### The Raoult law for concentrated solutions and transformation of sea haze droplets in the atmosphere of moist air

Let water vapor in atmospheric air be in contact with the volume phase of water solution along a plane surface. Assume that the thermodynamic system is in the thermostat  $T$  at fixed external pressure  $p$  being a sum of pressures of dry air and water vapor  $E$ .

Under conditions of thermodynamic equilibrium, the specific chemical potential of water vapor  $\phi_v$  is equal to the specific chemical potential of water in solution  $\phi_{WS}$ . Vapor in the system is at saturated pressure  $E$ , and hydrostatic pressure of water in solution is determined by external pressure  $p$ , which

decreases due to the osmotic pressure  $\pi^*$ . Finally, on the plane surface of the solution

$$\varphi_v(T, E) = \varphi_{ws}(T, p, \pi^*). \quad (11)$$

Let  $E_\infty^s$  be the pressure of saturated vapor above the plane surface of saturated solution with osmotic pressure  $\pi^*$ . Then the phase equilibrium condition (11) takes the form

$$\varphi_v(T, E_\infty^s) = \varphi_{ws}(T, p, \pi_\infty^*). \quad (12)$$

Subtracting Eq. (12) from Eq. (11), we obtain the main relationship

$$\begin{aligned} \varphi_v(T, E) - \varphi_v(T, E_\infty^s) &= \\ &= \varphi_{ws}(T, p, \pi^*) - \varphi_{ws}(T, p, \pi_\infty^*). \end{aligned} \quad (13)$$

Let us transform the right- and left-hand sides of Eq. (13) taking into account Eqs. (10), (6), and (9), then

$$\begin{cases} \varphi_v(T, E) - \varphi_v(T, E_\infty^s) = \int_{E_\infty^s}^E v_v dE = R_W T \ln \frac{E}{E_\infty^s}, \\ \varphi_{ws}(T, p, \pi^*) - \varphi_{ws}(T, p, \pi_\infty^*) = \int_{\pi_\infty^*}^{\pi^*} v_{ws} dp = \\ = K_\infty v_W (\pi^* - \pi_\infty^*) = j_\infty R_W T \ln \frac{C}{C_\infty}. \end{cases} \quad (14)$$

Finally, the phase equilibrium condition (13) takes the form of modified Raoult's law for concentrated and moderately supersaturated solutions

$$\ln \frac{E}{E_\infty^s} = j_\infty \ln \frac{C}{C_\infty}, \quad j_\infty = K_\infty i_\infty C_\infty. \quad (15)$$

The experimental values of dimensionless pressure of the saturated vapor above the NaCl solution and calculated by formula (15) are compared in Fig. 7. Vertical axis corresponds to the ratio of the pressure of the saturated vapor above  $E$  to the value of pressure of the saturated vapor above the plane surface of pure water  $E_\infty$ . The ratio of the number of moles of the dissolved salt to the total number of moles in the solution equal to  $c/(1+c)$  is plotted along the horizontal axis.

Let a solid particle of radius  $a$  be completely dissolved in the solution droplet of radius  $r$ . Then, according to the approximation of volume of saturated solution, the concentration  $c$  can be related to the solution droplet radius  $r$  by the formula

$$c_\infty/c = r^3/r_s^3, \quad (16)$$

where  $r_s$  is the radius of the saturated solution droplet at dissolving the solid particle of the radius  $a$  in water.

Taking into account Eq. (16) for large spherical droplets, above which the pressure of saturated vapor does not depend on the surface tension coefficient,

relationship (15) takes the following form of the modified Raoult law:

$$r^3/r_s^3 = (f/f_s)^{1/j_\infty}, \quad (17)$$

where  $r$  and  $r_s$  are the radii of the solution droplets at relative humidity  $f$  and relative humidity of saturation  $f_s$ , respectively.

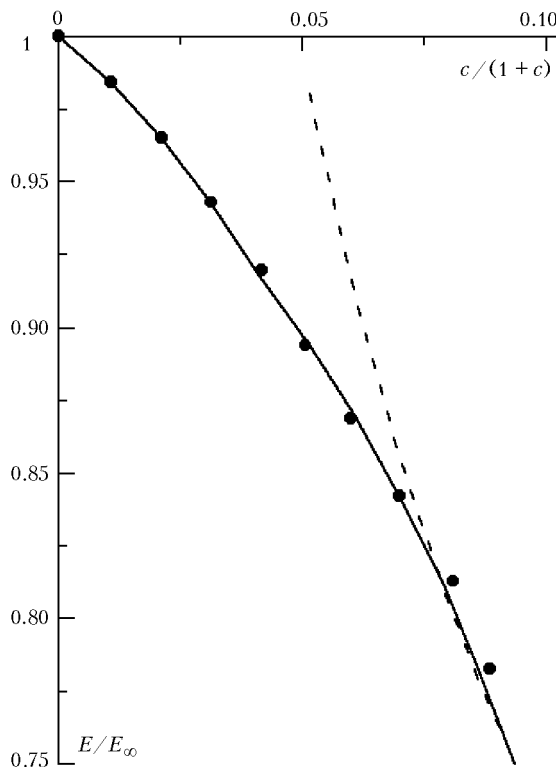


Fig. 7. Comparison of the dependences of experimental data on the pressure of saturated vapor over the solution of NaCl (solid line) and the values of the saturated vapor pressure calculated by formula (15) (dotted line).

Using Eqs. (5) and (17) and assuming that the sea atmospheric haze consists only of large droplets of solution, we obtain the dependence of the spectral aerosol extinction coefficient  $\alpha_\lambda$  in the transparency window B on relative humidity, similar to that considered in Ref. 4:

$$\alpha_\lambda(f) = \frac{\beta_0}{\lambda} \left( \frac{f}{f_s} \right)^{1/j_\infty}, \quad (18)$$

where  $\beta_0$  is the constant numerical parameter, and  $\lambda$  is the light wavelength.

Field observations<sup>1,5</sup> at fixed values of relative humidity and their approximation by the relationship (18) are shown in Fig. 7. The results of comparison show that the relationship (18) quite well corresponds to the experimental data in the moderate range of variation of humidity for the atmospheric transparency window B at  $0.48 \cdot 10^4 < \lambda < 0.76 \cdot 10^4$  cm.

### Acknowledgments

The author would like to thank G.I. Gorchakov and G.P. Kokhanenko for some constructive discussions.

### References

1. M.V. Kabanov, M.V. Panchenko, Yu.A. Pkhalagov, et al., *Optical Properties of Coastal Atmospheric Hazes* (Nauka, Novosibirsk, 1988), 201 pp.
2. B.D. Meison, *Cloud Physics* (Gidrometeoizdat, Leningrad, 1961), 542 pp.
3. H.L. Wright, *Quart. J. Roy. Meteorol. Soc.* **65**, 411\$426 (1939).
4. G. manel, *Adv. Geophys.* **19**, 73\$189 (1976).
5. V.E. Zuev, M.V. Kabanov, M.V. Panchenko, et al., *Izv. Akad. Nauk SSSR, Ser. Fiz. Atmos. Okeana* **14**, No. 12, 1268\$1274 (1978).
6. C. Orr, F.K. Hurd, W.P. Hendrix, and C. Junge, *J. Meteorol.* **15**, No. 2, 240\$242 (1958).
7. M. Born and E. Wolf, *Principles of Optics* (Nauka, Moscow, 1970), 856 pp.
8. A.N. Vulfson, *Izv. Akad. Nauk SSSR, Ser. Fiz. Atmos. Okeana* **34**, No. 2, 1\$8 (1998).
9. A.N. Vulfson, *Zh. Fiz. Khim.* **71**, No. 12, 2128\$2134 (1997).
10. Yu.I. Dytnerkii, *Reverse Osmosis and Ultrafiltration* (Khimiya, Moscow, 1978), 351 pp.
11. A.N. Vulfson, *Kolloidnyi Zh.* **53**, No. 2, 216\$222 (1991).
12. A.N. Vulfson, in: *Proceedings of International Conference on Physics of Atmospheric Aerosol (to 85th birthday of Prof. G.V. Rosenberg)* (Moscow, 1999).